J|A|C|S
ARTICLES
Published on Web 09/12/2006

Lanthanides to Quantum Dots Resonance Energy Transfer in Time-Resolved Fluoro-Immunoassays and Luminescence Microscopy

Loïc J. Charbonnière,*,† Niko Hildebrandt,*,‡ Raymond F. Ziessel,† and Hans-Gerd Löhmannsröben‡

Contribution from the Laboratoire de Chimie Moléculaire, UMR 7509 CNRS, ECPM 25 rue Becquerel, 67087 Strasbourg cedex 02, France, and Professur für Physikalische Chemie, Institut für Chemie und Interdisziplinäres Zentrum für Photonik, Universität Potsdam, Karl-Liebknecht-Str 24-25, 14476 Potsdam-Golm, Germany

Received April 18, 2006; E-mail: charbonn@chimie.u-strasbg.fr

Abstract: A time-resolved fluoro-immunoassay (TR-FIA) format is presented based on resonance energy transfer from visible emitting lanthanide complexes of europium and terbium, as energy donors, to semiconductor CdSe/ZnS core/shell nanocrystals (quantum dots, QD), as energy acceptors. The spatial proximity of the donor−acceptor pairs is obtained through the biological recognition process of biotin, coated at the surface of the dots (Biot−QD), and streptavidin labeled with the lanthanide markers (Ln−strep). The energy transfer phenomenon is evident from simultaneous lanthanide emission quenching and QD emission sensitization with a 1000-fold increase of the QD luminescence decay time reaching the hundred μs regime. Delayed emission detection allows for quantification of the recognition process and demonstrated a nearly quantitative association of the biotins to streptavidin with sensitivity limits reaching 1.2 pM of QD. Spectral characterization permits calculation of the energy transfer parameters. Extremely large Förster radii (R_0) values were obtained for Tb (104 Å) and Eu (96 Å) as a result of the relevant spectral overlap of donor emission and acceptor absorption. Special attention was paid to interactions with the varying constituents of the buffer for sensitivity and transfer efficiency optimization. The energy transfer phenomenon was also monitored by time-resolved luminescence microscopy experiments. At elevated concentration ($>10^{-5}$ M), Tb−strep precipitated in the form of pellets with long-lived green luminescence, whereas addition of Biot−QD led to red emitting pellets, with long excited-state decay times. The Ln−QD donor−acceptor hybrids appear as highly sensitive analytical tools both for TR-FIA and time-resolved luminescence microscopy experiments.

Introduction

The emergence of semiconductor nanocrystals or quantum dots (QDs) in the toolbox of fluorescence experiments[1] has opened ever increasing perspectives in fields such as analytical detection,[2] fluorescence microscopy,[3] or solar cells.[4] These nanoscaled building blocks display exceptional photophysical properties such as extremely high absorption cross sections, size dependent emission energies[5] with rather narrow emission bands, dependent on the size distribution of the dots, and sizable luminescence quantum yields approaching unity in some instances.[6] QDs display improved stability toward photobleaching, when compared to organic fluorophores,[7] and appear particularly efficient in high sensitivity techniques aiming at single molecule detection.[2b,8] Surface passivation[9] with shells of semiconducting material of larger band gap or chemical modification of the outer layers[10] likely improve their robustness and luminescence properties, and surface functionalization with polymers,[11] proteins,[12] peptides,[13] or hydrophilic molecules[14]

† Laboratoire de Chimie Moléculaire.
‡ Universität Potsdam.

(1) (a) Medintz, I.; Uyeda, H. T.; Goldman, E. R.; Mattoussi, H. *Nat. Mater.* **2005**, *4*, 435. (b) Green, M. *Angew. Chem., Int. Ed.* **2004**, *43*, 4129.
(2) (a) Medintz, I. L.; Clapp, A. R.; Mattoussi, H.; Goldman, E. R.; Fisher, B.; Mauro, J. M. *Nat. Mat.* **2003**, *2*, 630. (b) Chan, W. C. W.; Nie, S. *Science* **1998**, *281*, 2016.
(3) (a) Dubertret, B.; Skourides, P.; Norris, D. J.; Noireaux, V.; Brivanlou, A. H.; Libchaber, A. *Science* **2002**, *298*, 1759. (b) Michalet, X.; Pinaud, F. F.; Bentolila, L. A.; Tsay, J. M.; Doose, S.; Li, J. J.; Sundaresan, G.; Wu, A. M.; Gambhir, S. S.; Weiss, S. *Science* **2005**, *307*, 538. (c) Bharali, D. J.; Lucey, D. W.; Jayakumar, H.; Pudavar, H. E.; Prasad, P. N. *J. Am. Chem. Soc.* **2005**, *127*, 11364. (d) Green, M. *Angew. Chem., Int. Ed.* **2004**, *43*, 4129.
(4) (a) Gur, I.; Fromer, N. A.; Geier, M. L.; Alivisatos, A. P. *Science* **2005**, *310*, 462. (b) Grätzel, M. *Inorg. Chem.* **2005**, *44*, 6841.
(5) (a) Alivisatos, A. P. *Science* **1996**, *271*, 933. (b) Murray, C. B.; Norris, D. J.; Bawendi, M. G. *J. Am. Chem. Soc.* **1993**, *115*, 8706.
(6) (a) Reiss, P.; Bleuse, J.; Pron, A. *Nano Lett.* **2002**, *2*, 781. (b) Peng, X.; Schlamp, M. C.; Kadavanich, A. V.; Alivisatos, A. P. *J. Am. Chem. Soc.* **1997**, *119*, 7019.
(7) (a) Wu, X.; Liu, H.; Liu, J.; Haley, K. N.; Treadway, J. A.; Larson, J. P.; Ge, N.; Peale, F.; Bruchez, M. P. *Nat. Biotechnol.* **2003**, *21*, 41. (b) Jaiswal, J. K.; Mattoussi, H.; Mauro, J. M.; Simon, S. M. *Nat. Biotechnol.* **2003**, *21*, 47.
(8) Hohng, S.; Ha, T. *Chem. Phys. Chem.* **2005**, *6*, 956.
(9) Talapin, D. V.; Rogach, A. L.; Kornowslki, A.; Haase, M.; Weller, H. *Nano Lett.* **2001**, *1*, 207.
(10) Akamatsu, K.; Tsuruoka, T.; Nawafune, H. *J. Am. Chem. Soc.* **2005**, *127*, 1634.
(11) Potapova, I.; Mruk, R.; Hübner, C.; Zentel, R.; Basché, T.; Mews, A. *Angew. Chem., Int. Ed.* **2005**, *44*, 2437.
(12) Mamedova, N. N.; Kotov, N.; Rogach, A. L.; Studer, J. *Nano Lett.* **2001**, *1*, 281.

 10.1021/ja062693a CCC: $33.50

allows for their use in aqueous media which was originally mostly restricted to organic solvents.[15] Such surface functionalization also widens the scope of applications to chemical events at the surface. Using this approach, QDs appeared as attractive tools in the frame of fluorescence resonance energy transfer (FRET) processes, in which an energy donor component in its excited-state transfers its energy to an acceptor counterpart, providing these two entities are brought in close spatial proximity, for example, through a chemical association. Regarding their efficient excitation and good to excellent luminescence quantum yields, QDs have been largely used as energy donors in FRET experiments, where the recognition process was established, for example, by interaction of biotin and streptavidin[8,16] of nitriloacetic acid and oligohistidine containing proteins[16] or of maltose binding protein and saccharides.[2a,14b,16] Interestingly, in all these homogeneous assays in solution, the dots are exclusively used as the energy donor component.

The use of QDs as energy acceptors[17] potentially offers various perspectives such as the possibility of very large Förster radii, low detection limits, and multiplex analysis, with interest for a broad scope of scientists interested in ultrasensitive fluoroimmunoassays, in sensor design, in the study of interactions within very large molecules, and in biomedical analysis by high throughput screening.

Very few examples dealt with the use of QDs as energy acceptors, except in solid-state devices combining QDs of smaller size (higher energy emission band),[18] quantum wells,[19] or polymer based matrixes.[20] It has been postulated that energy transfer (ET) to QDs in solution should be achieved through tryptophane excitation in CdTe QDs conjugated to bovine serum albumin (BSA),[12] but a thorough study of Mattoussi and coworkers[21] showed that organic fluorophores such as Cy3 or AlexaFluor 488 were unable to generate ET to CdSe QDs. The authors attributed this lack of effectiveness to the very fast radiative deactivation of these donors compared to ET processes. To confirm their hypothesis, they also checked longer-lived triplet emitter complexes of ruthenium as donors. However, this approach remained inconclusive. In a recent work, it was finally demonstrated that terbium luminescent complexes with millisecond excited-state lifetimes are prone to be excellent energy donors for ET to QDs.[22]

Lanthanide ions emitting in the visible range, and in particular the trivalent europium and terbium ions, possess very particular photophysical properties,[23] among which are linelike emission bands with corresponding excited-state lifetimes that can reach the millisecond time scale.[24] The origin of such a long-lived excited-state is to be found in the $f-f$ nature of the electronic transitions, which are both spin and Laporte forbidden.[25a] This characteristic of lanthanide ions is paralleled to the drawback, that molar absorption coefficients of lanthanide $f-f$ electronic transitions are also very weak (often less than 1 $M^{-1}cm^{-1}$).[25b] This major inconvenience has been largely bypassed in luminescent lanthanide complexes chemistry by the development of the so-called "antenna effect".[26] The principle consists in embedding the lanthanide ion into a chromophoric organic ligand, the role of which is to absorb light and to transfer energy as efficiently as possible to the lanthanide,[27] and to protect the cations from solvent molecules, particularly water, known to nonradiatively deactivate the lanthanide excited states through low-energy O−H, N−H or C−H oscillators.[28] Some few luminescent lanthanide labels that can be covalently linked to bioorganic material have been described in the literature[29,30] and used in analytical applications,[31] for example, in time-resolved luminescence microscopy (TRLM)[32] or as energy donors in

(13) (a) Pinaud, F.; King, D.; Moore, H.-P.; Weiss, S. *J. Am. Chem. Soc.* **2004**, *126*, 6115. (b) Chen, F.; Gerion, D. *Nano Lett.* **2004**, *4*, 1827.

(14) (a) Warner, J. H.; Hoshino, A.; Yamamoto, K.; Tilley, R. D. *Angew. Chem., Int. Ed.* **2005**, *44*, 4550. (b) Mattoussi, H.; Mauro, J. M.; Goldman, E. R.; Anderson, G. P.; Sundar, V. C.; Mikulec, F. V.; Bawendi, M. G. *J. Am. Chem. Soc.* **2000**, *122*, 12142. (c) Uyeda, H. T.; Medintz, I. L.; Jaiswal, J. K.; Simon, S. M.; Mattoussi, H. *J. Am. Chem. Soc.* **2005**, *127*, 3870. (d) Gaponik, N.; Talapin, D. V.; Rogach, A. L.; Hoppe, K.; Shevchenko, E. V.; Kornowski, A.; Eychmüller, A.; Weller, H. *J. Phys. Chem. B* **2002**, *106*, 7177. (e) Querner, C.; Reiss, P.; Bleuse, J.; Pron, A. *J. Am. Chem. Soc.* **2004**, *126*, 11574.

(15) Crouch, D.; Norager, S.; O'Brien, P.; Park, J.-H.; Pickett, N. *Philos. Trans. R. Soc. London, Ser. A* **2003**, *361*, 297.

(16) (a) Geissbuehler, I.; Hovius, R.; Martinez, K. L.; Adrian, M.; Thampi, K. R.; Vogel, H. *Angew. Chem., Int. Ed.* **2005**, *44*, 1388. (b) Oh, E.; Hong, M.-Y.; Lee, D.; Nam, S. H.; Yoon, H. C.; Kim, H. S. *J. Am. Chem. Soc.* **2005**, *127*, 3270. (c) Clapp, A. R.; Medintz, I. L.; Mauro, J. M.; Fisher, B. R.; Bawendi, M. G.; Mattoussi, H. *J. Am. Chem. Soc.* **2004**, *126*, 301.

(17) Clapp, A. R.; Medintz, I. L.; Mattoussi, H. *Chem. Phys. Chem.* **2006**, *7*, 47.

(18) (a) Kagan, C. R.; Murray, C. B.; Bawendi, M. G. *Phys. Rev. B* **1996**, *54*, 8633. (b) Kagan, C. R.; Murray, C. B.; Nirmal, M.; Bawendi, M. G. *Phys. Rev. Lett.* **1996**, *76*, 1517.

(19) Achermann, M.; Petruska, M. A.; Kos, S.; Smith, D. L.; Koleske, D. D.; Klimov, V. I. *Nature* **2004**, *429*, 642.

(20) Anni, M.; Manna, L.; Cingolani, R.; Valerini, D.; Creti, A.; Lomascolo, M. *App. Phys. Lett.* **2004**, *85*, 18.

(21) Clapp, A. R.; Medintz, I. L.; Fischer, B. R.; Anderson, G. P.; Mattoussi, H. *J. Am. Chem. Soc.* **2005**, *127*, 1242.

(22) Hildebrandt, N.; Charbonnière, L. J.; Beck, M.; Ziessel, R. F.; Löhmannsröben, H.-G. *Angew. Chem., Int. Ed.* **2005**, *44*, 7612.

(23) Bünzli, J.-C. G.; Piguet, C. *Chem. Soc. Rev.* **2005**, *34*, 1048.

(24) See for examples: (a) Elhabiri, M.; Scopelliti, R.; Bünzli, J.-C. G.; Piguet, C. *J. Am. Chem. Soc.* **1999**, *121*, 10747. (b) Poole, R. A.; Bobba, G.; Cann, M. J.; Frias, J.-C.; Parker, D.; Peacock, R. D. *Org. Biomol. Chem.* **2005**, *3*, 1013. (c) Chatterton, N.; Bretonnière, Y.; Pécaut, J.; Mazzanti, M. *Angew. Chem., Int. Ed.* **2005**, *44*, 7595. (d) Petoud, S.; Cohen, S. M.; Bünzli, J.-C. G.; Raymond, K. N. *J. Am. Chem. Soc.* **2003**, *125*, 13324. (d) Charbonnière, L.; Ziessel, R.; Guardigli, M.; Roda, A.; Sabbattini, N.; Cesario, M. *J. Am. Chem. Soc.* **2001**, *126*, 4889.

(25) (a) Bünzli, J.-C. G. In *Lanthanide Probes in Life, Chemical and Life Sci.*; Bünzli, J.-C. G., Choppin, G. R., Eds.; Elsevier: Amsterdam, The Netherlands, 1989; p 228. (b) Görller-Walrand, C.; Binnemans, K. In *Handbook on the Physics and Chemistry of Rare Earths*; Gschneidner, K.A., Eyring, L., Jr., Eds.; North Holland: Amsterdam, The Netherlands, 1998; Vol. 25.

(26) (a) Weissmann, S. I. *J. Chem. Phys.* 1942, *10*, 214. (b) Sabbatini, N.; Guardigli, M.; Lehn, J.-M. *Coord. Chem. Rev.* **1993**, *123*, 201.

(27) (a) Latva, M.; Takalo, H.; Mukkala, V.-M.; Matachescu, C.; Rodriguer-Ubis, J. C.; Kankare, J. *J. Lumin.* **1997**, *75*, 149. (b) Steemers, F. J.; Verboom, W.; Reinhoudt, D. N.; van der Tol, E. B.; Verhoeven, J. W. *J. Am. Chem. Soc.* **1995**, *117*, 9408.

(28) (a) Horrocks, W. D. W., Jr.; Sudnick, D. R. *J. Am. Chem. Soc.* **1979**, *101*, 334. (b) Supkowski, R. M.; Horrocks, W. D. W., Jr. *Inorg. Chim. Acta* **2002**, *340*, 44. (c) Beeby, A.; Clarkson, I. M.; Dickins, R. S.; Faulkner, S.; Parker, D.; Royle, L.; de Sousa, A. S.; Williams, J. A. G.; Woods, M. *J. Chem. Soc., Perkin Trans.* 2 **1999**, 493. (d) Hebbink, G. A.; Reinhoudt, D. N.; van Veggel, F. C. J. M. *Eur. J. Inorg. Chem.* **2001**, 4101.

(29) (a) Hemmila, I.; Mukkala, V.-M. *Crit. Rev. Clin. Lab. Sci.* **2001**, *38*, 441. (b) Hemmilä, I.; Webb, S. *Drug Discovery Today* **1997**, *2*, 373. (c) Bazin, H.; Préaudat, M.; Trinquet, E.; Mathis, G. *Spectrochim. Acta A* **2001**, *57*, 2197. (d) Evangelista, R. A.; Pollak, A.; Allore, B.; Templeton, E. F.; Morton, R. C.; Diamandis, E. P. *Clin. Biochem.* **1988**, *21*, 173. (e) Chen, J.; Selvin, P. R. *Bioconj. Chem.* **1999**, *10*, 311. (f) Takkalo, H.; Hemmilä, I.; Sutela, T.; Latva, M. *Helv. Chim. Acta* **1996**, *79*, 789. (g) Galaup, C.; Couchet, J.-M.; Bedel, S.; Tisnès, P.; Picard, C. *J. Org. Chem.* **2005**, *70*, 2274. (h) Johansson, M. K.; Cook, R. M.; Xu, J.; Raymond, K. N. *J. Am. Chem. Soc.* **2004**, *126*, 16451. (i) Yuan, J.; Matsumoto, K.; Kimura, H. *Anal. Chem.* **1998**, *70*, 596.

(30) Weibel, N.; Charbonnière, L.; Guardigli, M.; Roda, A.; Ziessel, R. *J. Am. Chem. Soc.* **2004**, *126*, 4888.

(31) (a) Elbanowski, M.; Makowska, B. *J. Photochem. Photobiol., A* **1996**, *99*, 85. (b) Yam, V. W.-W.; Lo, K. K.-M. *Coord. Chem. Rev.* **1998**, *184*, 157. (c) Woods, M.; Kovacs, Z.; Sherry, A. D. J. *Supramol. Chem.* **2002**, *2*, 1.

(32) (a) Soini, E. J.; Pelliniemi, L. J.; Hemmilä, I. A.; Mukkala, V.-M.; Kankare, J. J.; Frödjman, K. *J. Histochem. Cytochem.* **1988**, *36*, 1449. (b) Marriott, G.; Heidecker, M.; Diamandis, E. P.; Yan-Marriott, Y. *Biophys. J.* **1994**, *67*, 957. (c) Beeby, A.; Botchway, S. W.; Clarkson, I. M.; Faulkner, S.; Parker, A. W.; Parker, D.; Williams, J. A. G. *J. Photochem. Photobiol., B* **2000**, *57*, 83. (d) Charbonnière, L.; Weibel, N.; Estournes, C.; Leuvrey, C.; Ziessel, R. *New J. Chem.* **2004**, *28*, 777.

luminescence resonance energy transfer (LRET) experiments.[33] In the later cases lanthanide tags are particularly interesting as the extremely long luminescence lifetime of these donors is reverberated into very slow deactivation of the acceptors excited state,[34] and by this way, organic fluorophore acceptors can luminesce over tens to hundreds of microseconds. Applying time-resolved acquisition techniques then allows for elimination of the spurious fluorescent signals and light scattering in the apparatus, with a concomitant increase of sensitivity.[24d] Among the various donor−acceptor couples studied with lanthanide complexes as donors, one of the most studied is probably that using the Eu(TBP) cryptate as donor and allophycocyanin (APC or XL665) as acceptor.[35]

Lanthanide complexes appear well suited as energy donors in ET experiments using QDs as acceptors, and we recently demonstrated that Tb complexes were successful in that approach.[22] In this contribution, we provide compelling evidence that not only Tb but also Eu complexes can be efficient energy donors. The effectiveness of three different lanthanide donors (one of Tb, two of Eu) was checked, and the Ln−QD systems were compared to the Eu(TBP)−APC system. Furthermore, the Tb−QD donor−acceptor system was monitored by TRLM allowing for visualization of the energy transfer process at the microscopic level.

Results and Discussion

Characterization of Lanthanide Labeled Streptavidin Bioconjugates as Energy Donors. The assay is based on the strong recognition process between biotin and streptavidin, known to be very efficient in biological media with a first dissociation constant of 10^{-13} M^{-1}.[36] Three different lanthanide complexes labeled to streptavidin (Ln−strep) were used as donors in the study, the europium and terbium complexes of **L**[30] and the europium complex of TBP, Eu(TBP) (Scheme 1).[37] The TBP cryptate is a macrobicyclic ligand incorporating the europium cation in the cavity of the cryptate on which one of the bipyridyl loops was functionalized for covalent grafting to streptavidin. This complex carries a +III charge which is generally compensated by the addition of fluoride anions. Ligand **L** is based on a glutamate skeleton N-functionalized with two anionic bipyridyl chromophoric units, and containing a pendant carboxylic acid function which can be activated into an NHS[30] or a sulfo-NHS[22] ester for coupling on amino residues present on proteins, providing neutral complexes. Labeling of streptavidin by Ln**L** complexes (Ln = Eu or Tb) was achieved in PBS buffer at pH 7.4. The labeled proteins, Ln**L**−strep, were further purified by extensive dialysis and characterized by UV−vis absorption spectroscopy and MALDI-TOF mass spectrometry.

Scheme 1. Chemical Structures of Ln Complexes Used as Energy Donors

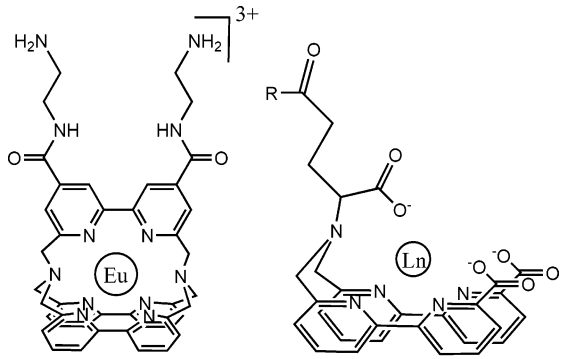

Eu(TBP) Ln**L**

Table 1. Main Photophysical Properties of the Lanthanide Complexes Used as Energy Donor (in Pure Water at 300 K).[30,37b]

	ϵ_{315nm} ($M^{-1}cm^{-1}$)	Φ^0_{ov} [a]	η_{sens} [b]	Φ^0_{Ln} [c]	τ^0_D [d]
Tb**L**[30]	18900	0.31	0.65	0.49	1480
Eu**L**[30]	17900	0.08	0.36	0.24	620
Eu(TBP)[37b]	18200	0.02	0.10	0.20	340

[a] Overall quantum yield (ligand excitation). [b] Ligand to metal energy transfer efficiency. [c] Lanthanide centered luminescence quantum yield. [d] Lanthanide luminescence lifetime in μs.

Assuming the absence of strong electronic perturbations owing to the labeling process, it was possible to quantify the labeling ratio, the number of complexes per streptavidin units, by deconvolution of the UV−vis spectra of the labeled streptavidin into a linear combination of the spectra of the pure label and pure protein (Figure S1, Supporting Information (SI)). For both Eu(TBP) and Tb**L**, labeling ratios close to 4 were obtained (4.1 and 3.7, respectively), meaning an average value of one label per monomeric unit comprising the tetrameric streptavidin protein. For Eu**L,** a poor labeling ratio of only 1.2 could be obtained. MALDI-TOF spectra of the three labeled streptavidin compounds and of unlabeled streptavidin are also presented in Figure S1 (SI). Streptavidin is composed of four monomeric subunits, and interestingly the spectra showed that the labeling process is not localized at a single position of the monomeric protein backbone. Besides unlabeled streptavidin monomers, proteins labeled with one complex are the predominant species for Ln**L**−strep, coexisting with minor amounts of double and triple labeled ones. For Eu(TBP)−strep single and double-labeled monomers are dominant. These spectra point to multiple possible environments for the lanthanide label.

Photophysical characterization of the labeled streptavidin compounds was accomplished by means of absorption spectroscopy as well as steady-state and time-resolved emission spectroscopy. Table 1 summarizes the main photophysical properties of the precursor lanthanide complexes[30,37] in pure water (denoted with a superscript 0), while emission spectra of the three Ln−strep derivatives are displayed in Figure 1.

Data of Table 1 indicate that all complexes display approximately the same absorption at the excitation wavelength of 315 nm, but that the overall quantum efficiency, Φ^0_{ov}, defined as the product of the ligand to lanthanide energy transfer efficiency (sensitization), η_{sens}, and of the lanthanide centered luminescence quantum yield, Φ^0_{Ln}, is largely in favor of Ln**L** complexes, particularly that of terbium. Nevertheless, these

(33) (a) Xiao, M.; Selvin, P. R. *J. Am. Chem. Soc.* **2001**, *123*, 7067. (b) Mathis, G. *J. Biomol. Screening* **1999**, *6*, 309. (c) Trinquet, E.; Maurin, F.; Preaudat, M.; Mathis, G. *Anal. Biochem.* **2001**, *296*, 232.
(34) (a) Valeur, B. In *Molecular Fluorescence, Principles and Applications*, Wiley-VCH: Weiheim, Germany, 2002. (b) Torelli, S.; Imbert, S.; Cantuel, M.; Bernardinelli, G.; Delahaye, S.; Hauser, A.; Bünzli, J.-C.G.; Piguet, C. *Chem.−Eur. J.* **2005**, *11*, 3228.
(35) See for example: (a) Gabourdes, M.; Bourgine, V.; Mathis, G.; Bazin, H.; Alpha-Bazin, B. *Anal. Biochem.* **2004**, *333*, 105. (b) Enomoto, K.; Nagasaki, T.; Yamauchi, A.; Onoda, J.; Sakai, K.; Yoshida, T.; Maekawa, K.; Kinoshita, Y.; Nishino, I.; Kikuoka, S.; Fukunaga, T.; Kawamoto, K.; Numata, Y.; Takemoto, H.; Nagata, K. *Anal. Biochem.* 2006, *351*, 229. (c) Mathis, G. *Clin. Chem.* **1993**, *39*, 1953.
(36) (a) Green, N. M. *Adv. Protein Chem.* **1975**, *29*, 85. (b) Loosli, A.; Rusbandi, U. E.; Gradinaru, J.; Bernauer, K.; Schlaepfer, C. W.; Meyer, M.; Mazurek, S.; Novic, M.; Ward, T. *Inorg. Chem.* **2006**, *45*, 660.
(37) (a) Alpha, B.; Lehn, J.-M.; Mathis, G. *Angew. Chem., Int. Ed. Eng.* **1987**, *26*, 266. (b) Alpha, B.; Ballardini, R.; Balzani, V.; Lehn J.-M.; Perathoner, S.; Sabbatini, N. *Photochem. Photobiol.* **1990**, *52*, 299−306.

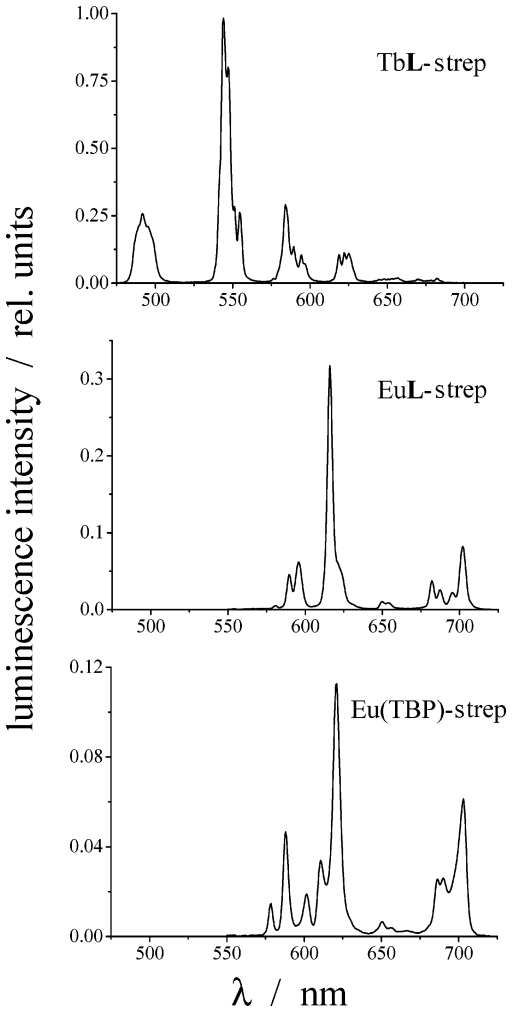

Figure 1. Emission spectra of the three lanthanide labeled streptavidin derivatives (borate buffer, pH 8.3, 2% BSA, 0.05% NaN_3, $\lambda_{exc} = 320 \pm 2$ nm, [strep] = 2 to 4 × 10^{-7} M).

results must be moderated by the fact that Φ^0_{Ln}, which is to be taken into account for the calculation of energy transfer parameters,[33a,47] did only vary by a factor 2.5 within the series. In order to estimate the possible influence of the different constituents of the assay medium on the donor properties, we systematically investigated the variations of the lanthanide centered luminescence lifetime, τ_D, for the three different Ln labeled streptavidin compounds in the presence of the borate buffer, of BSA and of added sodium azide. The presence of potassium fluoride (KF) was also tested, as fluoride anions are known to have a dramatic influence on the luminescence properties of lanthanide complexes in general[38] and on charged macropolycyclic cryptates such as Eu(TBP) in particular.[39] This hard lanthanophilic anion is able to compete with water and other anionic species and to alleviate their negative impact on the luminescence of lanthanides. τ_D values thereby obtained were then used to calculate Φ_{Ln} in the different conditions with eq 1 which results from eq 2,[40] assuming that the radiative (or intrinsic) lifetime τ_{rad} of each complex is independent of the medium:

$$\Phi_{Ln} = \Phi^0_{Ln} \times \frac{\tau_D}{\tau^0_D} \quad (1)$$

$$\tau_{rad} = \frac{\tau_D}{\Phi_{Ln}} \quad (2)$$

Regarding this equation, it was found that the different buffering media also have an influence on η_{sens} with a concomitant change of Φ_{ov}. As the donor in the RET process is the lanthanide ion itself, the altered η_{sens} has no impact on RET. Nevertheless, it has to be taken into account for the immunoassay efficiency and detection limit, respectively, because it leads to variable amounts of energy available for RET. Measured decay times and calculated quantum yields in the various media are summarized in Table T1 (SI).

From the results of Table T1, one can clearly see that Eu**L**−strep is very little influenced by borate, BSA, or NaN_3. In contrast, KF greatly increased the luminescence lifetime and quantum yields, as expected by the replacement of the water molecule in the first coordination sphere with a fluoride anion.[38,39] For Tb**L**−strep, while borate buffer and BSA has only minor effects, a surprising decrease of τ_D was observed upon the addition of NaN_3, which is used in biological buffers as antibacterial agent. This effect was further confirmed by titration experiments following the azide quenching effect as a function of added anions (Figure S2, SI). Such titrations also showed that at high Tb**L**−strep concentrations a biexponential luminescence decay could be found for azide concentrations of 0.05% and higher (Figure S3, SI), as observed in previous experiments.[22] The quenching effect of N_3^- anions on lanthanide luminescence has already been documented,[41] but it was reported to be far more efficient for Eu than for Tb. We thus attribute these variations to first coordination sphere perturbations.[42] Tb**L** provides a relatively small energy difference between the ligand centered triplet state and the Tb $^5D_4$ emitting level which only amounts to 1700 cm^{-1}.[30] This value is close to the limit value of 1850 cm^{-1} defined by Latva and co-workers,[27a] and subtle changes in the coordination sphere of Tb may improve the energy back transfer processes from Tb^{3+} to the ligand. Interestingly, fluoride anions strongly enhanced the luminescence lifetime of Tb, nearly reaching values obtained in pure D_2O,[30] and in the presence of all buffer constituents the combined effects of NaN_3 and KF are compensated to afford values similar to that in pure water. Unlike the other complexes, Eu(TBP)−strep luminescence shows an obvious two-exponential decay behavior (decay times τ_{D1} and τ_{D2}) in water as well as in borate buffer with or without NaN_3, likely because of the presence of two distinct emitting species. Concerning Eu(TBP)−strep, the major influence is as expected due to fluoride anions, which removed water from the first coordination sphere and resulted in a monoexponential luminescence decay.

Photophysical Characterization of the Energy Acceptors. The energy acceptor modules (Biot−QD) were composed of

(38) (a) Tsukube, H.; Shinoda, S. *Chem. Rev.* **2002**, *102*, 2389. (b) Charbonnière, L.; Ziessel, R.; Montalti, M.; Prodi, L.; Zaccheroni, N.; Boehme, C.; Wipff, G. *J. Am. Chem. Soc.* **2002**, *124*, 7779.
(39) Mathis, G. *Clin. Chem.* **1988**, *34*, 1163.
(40) (a) Werts, M. H. V.; Jukes, R. T. F.; Verhoeven, J. W. *Phys. Chem. Chem. Phys.* **2002**, *4*, 1542. (b) Chauvin, A.-S.; Gumy, F.; Imbert, D.; Bünzli, J.-C. G. *Spectrosc. Lett.* **2004**, *37*, 517.
(41) Lis, S.; Kimura, T.; Yoshida, Z. *J. Alloys Compd.* **2001**, *323*, 125.
(42) Blasse, G.; Dirksen, G. J.; Sabbatini, N.; Perathoner, S.; Lehn, J. M.; Alpha, B. *J. Phys. Chem.* **1988**, *92*, 2419−2422.

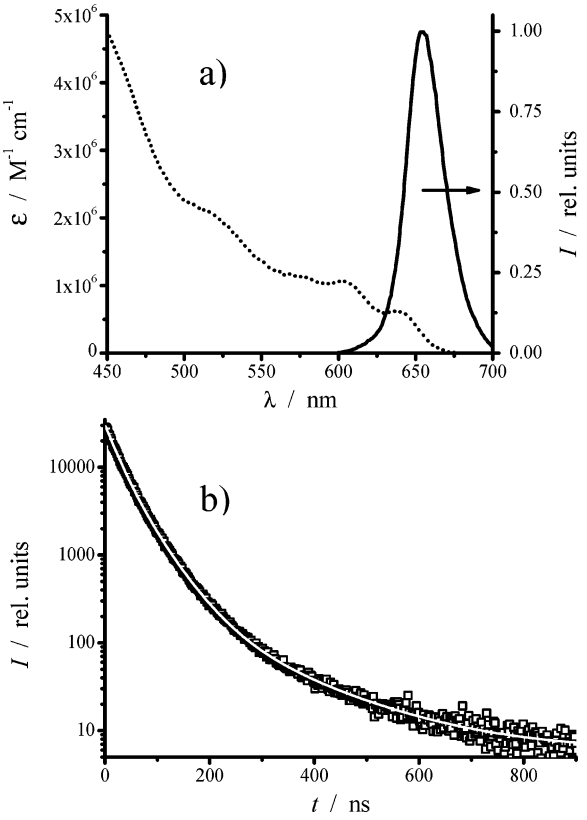

Figure 2. (a) Absorption (dots) and emission spectra of Biot−QD (50 mM borate buffer, pH 8.3, 2% BSA, 0.05% NaN_3); (b) luminescence decay (from 625−685 nm integrated intensity *I*) of Biot−QD (50 mM borate buffer, pH 8.3, 2% BSA, 0.05% NaN_3, $\lambda_{exc} = 308$ nm) with decay times of 23 ns (41%), 47 ns (53%) and 160 ns (6%).

Scheme 2: Structure of Biotinylated CdSe/ZnS Core/Shell Nanocrystals, Biot-QD, Containing an Average of Six Biotin Molecules at Their Surface (Biotin Molecules Not at Scale)

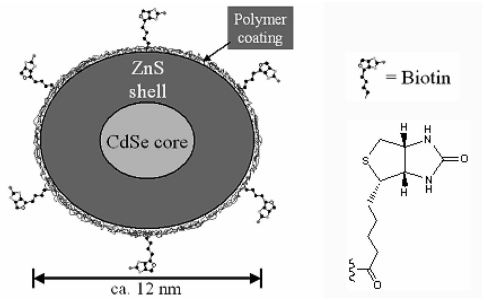

QD655,[43] CdSe/ZnS semiconductor nanocrystals coated with a polymer shell containing 5 to 7 biotin molecules per dot at their surface (Scheme 2). Absorption and emission spectra of Biot−QD in their buffer are presented in Figure 2a, and confirmed the very large absorption cross sections together with a narrow emission band culminating at 655 nm.

The luminescence decay in the same medium is shown in Figure 2b. It could be conveniently fitted by using multiexponential behavior and showed two main short-lived components of 23 and 47 ns. This behavior is commonly observed for the luminescence decay of nanocrystals and arises from the size distribution of the QDs and their anisotropy.[44]

Resonance Energy Transfer Experiments. RET experiments were realized by stepwise addition of increasing amounts

(43) *Qdot Biotin Conjugates User Manual* (cat. no. 1030-1, cat. no. 1032-1); www.qdots.com.

Scheme 3. Schematic Representation of Ln−strep Complexes Before (Left) and After Addition of Biot−QD (Diameter of a Ln−Strep Complex is Approximately 6 nm)

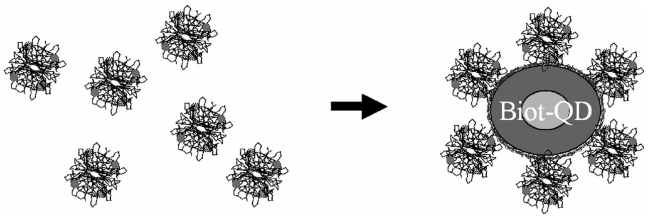

of biotinylated acceptor into a solution containing the lanthanide labeled streptavidin in borate buffer at pH 8.3 with 2% BSA and 0.05% NaN_3. A graphic describing the case of titration of Ln**L**−strep by Biot−QD is sketched in Scheme 3.

After each addition of aliquots, time-resolved emission spectra of the solution were recorded upon excitation at 308 nm (maximum excitation of Tb**L**) and after a delay δ of 250 μs and for an integration window ω of 750 μs. The integration parameters were chosen so as to get rid of the residual prompt fluorescence of the acceptor and of the buffering medium. It is first to be noted that after each addition the system slowly evolved in time, and the equilibrium was only reached after at least 1 h at this concentration ([Tb**L**−strep] = 2.7×10^{-7} M). Figure 3 shows the evolution of the gated emission spectra normalized on Tb emission at 545 nm, obtained upon titration of Tb**L**−strep by Biot−QD in the experimental conditions cited above after the equilibrium was reached. For molar ratios of 0 to 0.18 Biot−QD per streptavidin, the time-resolved spectra showed the appearance of a new band with intensity maximum at 655 nm which slowly increases with Biot−QD concentration. For molar ratios larger than 0.18, the gated emission spectra did not evolve anymore. From its shape and energy maximum, the new emission band arising at 655 nm was assigned to QD emission owing to RET from Tb complexes. The possibilities of direct excitation of the dots or dynamic RET occurring in solution were ruled out by control experiments in which the same gated emission spectra were recorded for solutions of Biot−QD and free Tb**L** complexes in the same concentration ranges and for up to 100-fold excess of free Tb**L**. In these

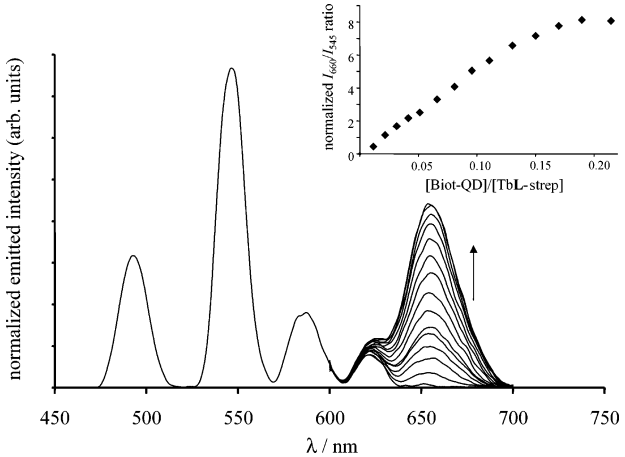

Figure 3. Evolution of the gated emission spectra ($\lambda_{exc} = 308$ nm, $\delta = 0.25$ ms, $\omega = 0.75$ ms) upon addition of increasing amounts of Biot−QD to a solution of Tb**L**−strep ($c = 2.7 \times 10^{-7}$ M, borate buffer pH 8.3, 2% BSA, 0.05% NaN_3). Spectra were normalized on Tb emission at 545 nm. Inset: Normalized intensity ratio for emission at 660 nm (Biot−QD) and 545 nm (Tb**L**−strep) as a function of added Biot−QD.

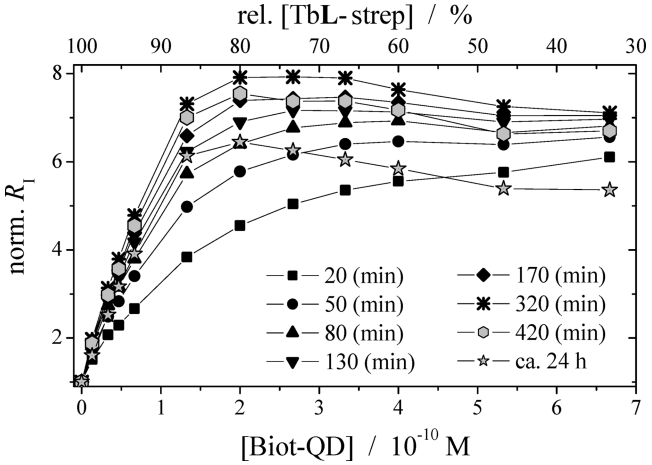

Figure 4. Kinetic evolution of the normalized intensity ratio R_I as a function of [Biot−QD] (borate buffer pH 8.3, 2% BSA, 0.05% NaN_3, starting concentration [Tb**L**−strep] = 1.0×10^{-9} M).

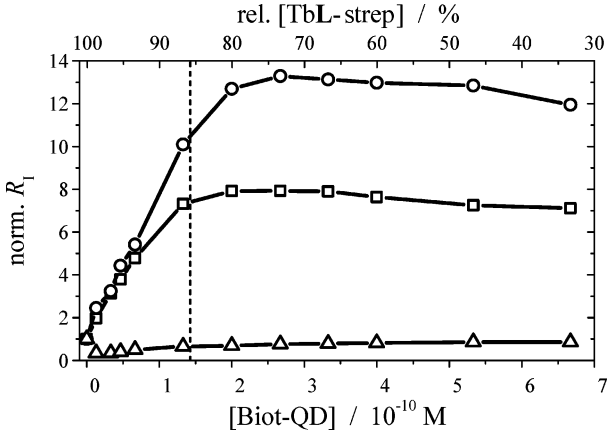

Figure 5. Evolution of R_I as a function of [Biot−QD] added to Tb**L**−strep in pure borate buffer pH 8.3 after 7 h incubation time (buffer A, triangles); borate buffer pH 8.3, 2% BSA and 0.05% NaN_3 after 5 h (buffer B, squares); borate buffer pH 8.3, 2% BSA, 0.05% NaN_3 and 0.5 M KF after 4 h (buffer C, circles). Starting concentration [Tb**L**−strep] = 1.0×10^{-9} M. The dotted line indicates a ratio of 6 Tb**L**−strep per Biot−QD.

controls, no new emission band could be observed at 655 nm, unambiguously confirming that the long-lasting emission of QD is a result of RET from the terbium complex.

The evolution of the RET process can be followed by the ratio of the normalized emission of QD to that of Tb (inset in Figure 3). As a result of a non-negligible emission of Tb at 655 nm (weak $^5D_4 \rightarrow {}^7F_2$ transition), the emission of QD was preferentially measured at 660 nm and normalized to that of the main emission band of Tb ($^5D_4 \rightarrow {}^7F_5$ transition at 545 nm). The intensity ratio linearly increased up to a molar ratio of 0.18 Biot−QD per Tb**L**−strep and remained nearly unchanged at higher ratio. This ratio corresponds to 5.6 streptavidin molecules linked to the QDs and is in excellent agreement with the number of biotin molecules linked to the surface of QDs certified by the supplier (5 to 7).

Further insights into the RET experiments were obtained by automated titration experiments made on a modified KRYPTOR system, equipped with well plate readers, using laser excitation at 315 nm (see Experimental Section). Time gated (250−1000 μs) emission intensities I at (545 ± 5) (Tb) and (665 ± 5) (QD)[45] nm were recorded, and the normalized ratio $R_I = I_{665}/I_{545}$ was plotted against Biot−QD concentration. In order to follow the decrease of Tb**L** concentration caused by dilution with Biot−QD a second x-coordinate with relative Tb**L**−strep concentration is also displayed. By this means it was possible to follow the entire kinetic evolution of the system at low concentrations of reactants (typically 10^{-10} M) and to monitor the influence of the constituents of the buffering media on the assay efficiency. Figure 4 represents the kinetic profiles observed in borate buffer containing BSA and NaN_3 from which it appeared that at such low levels of streptavidin the assay took at least 5 h to be fully equilibrated. This very slow kinetic equilibration was attributed to the presence of large amounts of BSA, known to create nonspecific binding with streptavidin.[46] Before the streptavidin−biotin recognition process can occur, the BSA must first be "peeled off" from streptavidin, a process which takes a few hours.

To compare the different buffering conditions on the assay efficiency, three different buffers were investigated. The first one, buffer A, consisted of the 50 mM borate, pH 8.3. In this case, it must nevertheless be kept in mind that the added commercial solution of Biot−QD contains both BSA (2%) and NaN_3 (0.05%). The second one, buffer B, contained all the constituents of the Biot−QD mother solution : 2% BSA in 50 mM borate, pH 8.3 with 0.05% sodium azide. Finally, buffer C is the same as buffer B plus 0.5 M potassium fluoride. The results obtained for the evolution of the normalized values of R_I as a function of added Biot−QD after the optimal equilibration time are plotted in Figure 5. Similar evolutions are observed for buffers B and C, with R_I climbing rapidly until the [Biot−QD]/[Tb**L**−strep] ratio reached a value of approximately $^1/_6$, in good agreement with the number of biotin molecules per QD (5 to 7). For larger [Biot−QD], R_I remained stable to a plateau value. Noteworthy, the presence of KF into the assay (buffer C) significantly increased the measured intensity ratio, as expected on the basis of the observed influence of KF on the Tb**L** luminescence efficiency (Table T1, SI). A surprising result was observed for buffer A. In the absence of BSA and NaN_3, the intensity ratio was first observed to drop dramatically for the very first aliquots of added [Biot−QD] solutions before it increased again. Careful examination of the data showed this drop to be due to a very large increase of the intensity of the Tb emission. Regarding the negative impact of NaN_3 on the luminescence efficiency of Tb (Table T1), this behavior was tentatively attributed to the BSA present in the Biot-QD buffer. To confirm this hypothesis, a titration was performed in which increasing amounts of BSA were added to the solution containing Tb**L**−strep or Eu**L**−strep. The results, displayed in Figure S4 (SI) showed that in both cases the lanthanide luminescence largely increased after an incubation time of 5 h. This phenomenon was attributed to the use of polystyrene (PS) well plates in our measuring setup, where adsorption of proteins occurs owing to hydrophobic binding. At such low concentrations (10^{-9} to 10^{-10} M) streptavidin is adsorbed to the PS walls

(44) (a) Chan, W. C. W.; Maxwell, D. J.; Gao, X.; Bailey, R. E.; Han, M.; Nie, S. *Cur. Opin. Biotechnol.* **2002**, *13*, 40. (b) Schlegel, G.; Bohnenberger, J.; Potatova, I.; Mews, A. *Phys. Rev. Lett.* **2002**, *88*, 137401. (c) Fischer, B. R.; Eisler, H. J.; Stott, N. E.; Bawendi, M. G. *J. Phys. Chem. B* **2004**, *108*, 143.
(45) In that case, the chosen wavelength was 665 nm for simple practical filtering considerations.
(46) Erkens, J. H. F.; Dieleman, S. J.; Dressendörfer, R. A.; Strasburger, C. J. *J. Steroid Biochem. Molec. Biol.* **1998**, *67*, 153.

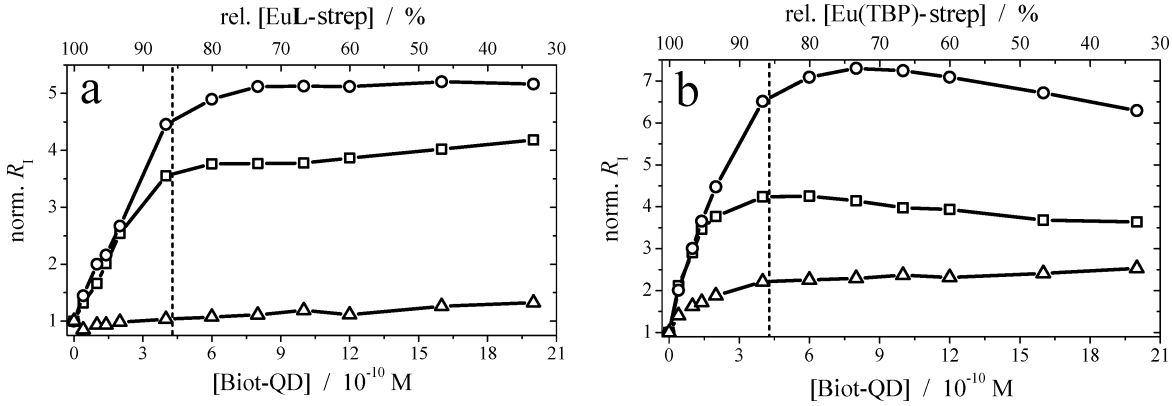

Figure 6. Evolution of R_I for (a) (Eu**L**−strep)−(Biot−QD) and (b) (Eu(TBP)−strep)−(Biot−QD) as a function of [Biot−QD] in buffer A (triangles), in buffer B (squares), and in buffer C (circles). Starting concentrations [Eu**L**−strep] = [Eu(TBP)−strep] = 3×10^{-9} M. The dotted line indicates a ratio of 6 strep per Biot−QD.

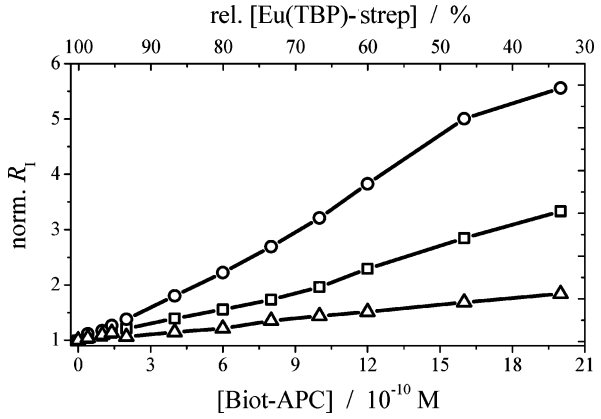

Figure 7. Evolution of R_I as a function of [Biot−APC] added to Eu(TBP)−strep in buffer A (triangles), in buffer B (squares), and in buffer C (circles). Starting concentration [Eu(TBP)−strep] = 3×10^{-9} M.

of the well plate and addition of BSA allowed for desorption of the protein. This hypothesis was further confirmed by similar experiments ran with Eu**L**−strep and Eu(TBP)−strep (vide infra).

Having in hands the optimum conditions for the assay experiment, the lanthanide to QD energy transfer process was checked with europium as a donor using Eu**L**−strep and Eu(TBP)−strep. In these cases, the long-lived emission intensities were measured from 250 to 1000 μs at 620 ± 5 nm for the Eu and at 665 ± 5 nm for the dots. The intensitiy ratios, $R_I = I_{665}/I_{620}$, were measured for each aliquot of added Biot−QD, normalized, and plotted as a function of Biot−QD concentration. The results obtained in buffers A to C are collected in Figure 6. In these two cases, preliminary experiments showed that the concentrations of Eu**L**−strep and Eu(TBP)−strep, as well as that of Biot−QD had to be chosen at least 3 times higher than with Tb**L**−strep to generate sufficient and comparable emission signals. In the cases of buffers B and C, a new long lasting emission can be evidenced in the QD channel, pointing to RET from the Eu complexes to QD upon excitation at 315 nm. As observed for Tb, the evolution of R_I showed a sharp increase for the [Biot−QD]/[Ln−strep] ratio smaller than $^1/_6$ and a plateau region for larger values. The cases of buffer A are very informative. For BSA free solution of Eu**L**−strep, addition of BSA containing aliquots of Biot−QD led first to a drop of R_I, because of an increase of luminescence in the Eu channel. This behavior is similar to that of Tb**L**−strep and was explained by adsorption of BSA on the polystyrene walls. In contrast, the phenomenon could not be observed for Eu(TBP)−strep (Figure 6b), which was supplied in a BSA containing buffer. This unambiguously corroborated the influence of BSA on the adsorption phenomena and justified the use of BSA in the assay.

In order to compare these results to the often analytically applied and very sensitive Eu(TBP)−APC system[35,37] the same measurements were performed with Eu(TBP)−strep as donor and biotinilated APC (Biot−APC) as acceptor (Figure 7). The steeply rising intensity ratio found for Biot−QD as acceptor cannot be found for Biot−APC, where the slope is rather flat. Furthermore a saturation of the (Eu(TBP)−strep)−(Biot−APC) binding is not reached within the concentration range of the measurement supposing that only a few of the biotin molecules (10 to 15 per APC) are accessible for Eu(TBP)−strep. Nevertheless the rising slopes of normalized R_I over Biot−APC concentration indicate RET from Eu(TBP) to APC.

For all the measurements QD as well as APC direct excitation and dynamic RET were ruled out by control experiments using free lanthanide complexes with Biot−QD and Biot−APC, respectively (see Figure S5−S8, SI).

The linear part of the curves for buffer B and C ([Biot−QD]/[Ln−strep] < $^1/_6$) was used for the calculation of the limit of detection (LOD) using eq 3 with σ_0 being the standard deviation (for 10 measurements) of R_I at [Biot−QD] = 0.

$$\mathrm{LOD} = 3\sigma_0\Delta[\text{Biot−QD}]/\Delta R_I \qquad (3)$$

For comparison, all detection limits obtained in buffer B and C are summarized in Table 2. LODs for Biot−QD of (1.6 ± 0.6) × 10^{-12} M in buffer B and (1.2 ± 0.5) × 10^{-12} M in buffer C could be achieved using this type of streptavidin-biotin binding immunoassay with Tb**L** as donor. The large benefit of using QD as energy acceptor in combination with Tb**L** as donor is clarified by a sensitivity improvement of more than 1 order of magnitude compared to LODs accomplished for the Eu(TBP)−APC system, namely (71 ± 12) × 10^{-12} M in buffer B and (24 ± 12) × 10^{-12} M in buffer C, respectively. It has to be noted that the immunoassay is not totally optimized so that technical (laser, detectors, etc.) as well as chemical (concentration ratios, labeling, etc.) modifications can further improve the LODs in order to obtain femtomolar detection.

Theoretical Treatment and RET Efficiency Parametrization. Calculation of the Förster Radii. Using the calculated

Table 2. Measured Decay Times τ, LODs, and Calculated RET Parameters R_0, r, k_{ET} and E for the Three Ln−Strep Donors in the Different Buffers

	Tb**L**–strep			Eu**L**–strep			Eu(TBP)–strep		
buffer[a]	A	B	C	A	B	C	A	B	C
τ_{D1} (μs)	1100 ± 50	620 ± 30	1360 ± 50	650 ± 30	680 ± 30	1400 ± 60	660 ± 30	1050 ± 50	1100 ± 30
τ_{D2} (μs)							220 ± 30	230 ± 30	
R_0 (Å)	96 ± 3	85 ± 4	98 ± 2	84 ± 2	85 ± 2	96 ± 2	84 ± 2	90 ± 2	92 ± 2
τ_{DA1} (μs)	570 ± 30	410 ± 30	440 ± 20	*b*	490 ± 20	680 ± 20	410 ± 50	400 ± 40	700 ± 20
τ_{DA2} (μs)				*b*			130 ± 30	90 ± 20	
r (Å)	97 ± 3	95 ± 3	87 ± 2	*b*	100 ± 3	95 ± 2	91 ± 4	83 ± 4	101 ± 2
k_{ET1} (s^{-1})	850 ± 100	830 ± 100	1500 ± 50	*b*	560 ± 70	760 ± 30	880 ± 100	1550 ±200	520 ± 40
k_{ET2} (s^{-1})				*b*			2650 ± 200	7100 ± 200	
E (%)	48 ± 4	34 ± 4	67 ± 2	*b*	27 ± 4	52 ± 2	36 ± 5	62 ± 5	36 ± 5
LOD (pM)	*b*	1.6 ± 0.6	1.2 ± 0.5	*b*	12 ± 4	8 ± 2	*b*	4 ±1	2.6 ± 1.4

[a] Buffer A: 50 mM borate, pH 8.3. Buffer B: 50 mM borate, pH 8.3 with 2% BSA and 0.05% sodium azide. Buffer C: 50 mM borate, pH 8.3 with 2% BSA, 0.05% sodium azide and 0.5 M potassium fluoride. [b] Too low signals for an accurate determination.

quantum yields Φ_{Ln} (Table 1, and eq 2) the normalized donor luminescence spectrum, $I_D(\lambda)$ (Figure 1), and the acceptor absorption spectrum $\epsilon_A(\lambda)$ (Figure 2), the Förster radii R_0 for the different donor−acceptor pairs become accessible with the calculation of the overlap integral J_λ using the following equations:[47]

$$J_\lambda = \int_0^\infty \epsilon_A(\lambda)\, I_D(\lambda)\, \lambda^4\, d\lambda \tag{4}$$

$$R_0 = [(8.79 \times 10^{-5})\kappa^2 \Phi_{Ln} n^{-4} J_\lambda]^{1/6} \tag{5}$$

with a refractive index of $n = 1.4$ for biomolecules in aqueous solution[47] and a dipole orientation factor of $\kappa^2 = {}^2/_3$ that took into account a statistical distribution of the donor−acceptor dipoles within the luminescence decay time of the donor.[48] The calculated values in different buffers are summarized in Table T2 (SI). Pure water as solvent was not taken into account, as Biot−QD is not stable inside this medium. R_0 values for the buffers containing sodium azide are given in Table 2.

As a result of the high $\epsilon(\lambda)$ for qdots and the good spectral overlap with the lanthanide complexes, the R_0 values are considerably larger than the ones of conventional donor−acceptor pairs (with distances ranging from 21−61 Å)[34a] or pairs containing qdots as donors (39−65 Å).[16a,17,51] Even the very high Förster radii of the Eu(TBP)−APC system under ideal conditions (approximately 90 Å in phosphate buffer)[35c] and unbound donor−acceptor pairs (71−98 Å)[48] are lower than the Tb**L**−QD values with 96 to 104 Å (Table T2, SI).

Energy Transfer Parameters. Within the frame of the theory of resonance energy transfer developed by Förster,[49] and assuming the possibility of multiple lanthanide donor species in the system, the time and donor−acceptor distance dependence of the luminescence intensity of the donors in the presence of the acceptor, $I_{DA}(r, t)$, can be described by equation 6,[47] in which τ_{Di} are the donor decay times in absence of acceptor and R_0 the Förster radius for the donor−acceptor system considered:

$$I_{DA}(r, t) = \sum_i \alpha_{Di} \exp\left[-\frac{t}{\tau_{Di}} - \frac{t}{\tau_{Di}}\left(\frac{R_0}{r}\right)^6\right] \tag{6}$$

with α_{Di} being the pre-exponential factors for each *i*th decay-time component and r the distance between donor and acceptor. Equation 6 becomes simple for the Ln**L**−strep donors with monoexponential decays and only slightly more complicated in the case of the Eu(TBP)−strep donor in buffer A and B with two-exponential decay behaviors.

The intrinsic Biot−QD decay being very prompt compared to the luminescence decay of the lanthanide ions, the long-lived Biot−QD luminescence in the presence of Ln−strep is due to the fraction x of the energy of the donor transferred to the acceptor, $xI_{DA}(r, t)$, characterized by a decay time τ_{DA}.[34] The overall emission intensity at the QD channel, $I_{QD}(r, t)$, is then the sum of the acceptor emission resulting from RET plus a background emission I(background), emanating from nontransferring lanthanide donors (especially for europium), parasitic emission from the measurement apparatus (light scattering, fluorescence from the well plate reader), and from short-lived Biot−QD fluorescence which appears partly as a pseudo-long-lived component due to a saturation of the photomultipliers (working at 1.2 kV) in the short-time scale.

$$I_{QD}(r, t) = I(\text{background}) + xI_{DA}(r,\ t) \tag{7}$$

From the measurement of I(background) obtained in the absence of acceptor, $I_{QD}(r, t)$ allowed for fitting of r and then for calculation of the energy transfer rates k_{ETi} , for the lifetimes τ_{DAi} of each donor in the presence of acceptor, as well as for the RET efficiency E using equations 8 to 10.[47] The results are gathered in Table 2, together with values of the limit of detection previously obtained.

$$k_{ETi} = \left(\frac{1}{\tau_{Di}}\right)\left(\frac{R_0}{r}\right)^6 \tag{8}$$

$$\frac{1}{\tau_{DAi}} = \frac{1}{\tau_{Di}} + k_{ETi} \tag{9}$$

$$E = \frac{{R_0}^6}{{R_0}^6 + r^6} \tag{10}$$

The resulting average donor−acceptor distances are in the range of 83−101 Å, which is in good agreement with the binding model depicted in Scheme 3, with the structural parameters of the nanocrystals (ellipsoidally shaped with 100−120 Å length along the main axis),[43] and with streptavidin in

(47) Lakowicz, J. R. *Principles of Fluorescence Spectroscopy*; Kluwer Academic/Plenum Publishers: New York, 1999.
(48) Selvin P. R. *Annu. Rev. Biophys. Biomol. Struct.* **2002**, *31*, 275.
(49) Förster, Th. *Ann. Phys.* **1948**, *2*, 55.

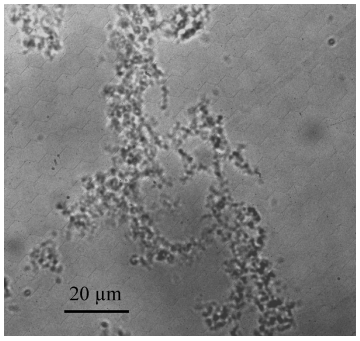

Figure 8. Transmission micrograph of the aggregates formed upon buffering a concentrated solution of Tb**L**−strep in water (×100) to pH 8.3.

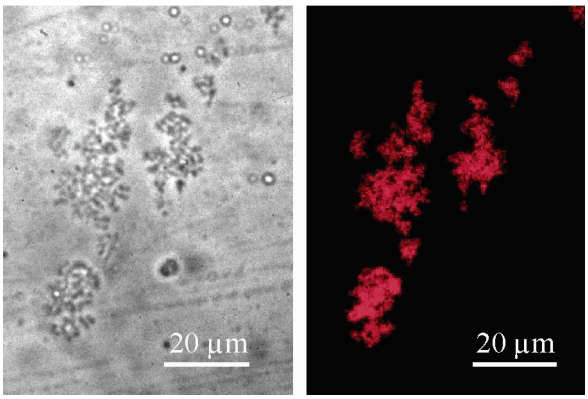

Figure 9. Transmission (left, ×100 magnification) and fluorescence micrographs (right, ×40 magnification, $300 < \lambda_{exc} < 350$ nm) of the aggregates of Tb**L**−strep after incubation of Biot−QD (bar scale: 20 μm).

the solid state ($54 \times 58 \times 48$ Å^3).[50] A noticeable exception arose with Eu(TBP) in absence of KF (buffer A and B), where a shorter 83−91 Å distance is observed. In that particular case, the charged Eu complexes may provide particular electrostatic interactions with Biot−QD that shortened the distance.

For Ln**L**−strep the best RET efficiencies as well as LODs could be achieved for buffer C because of both higher Förster radii and energy transfer rates. The best LODs were obtained for Tb**L** resulting from a combination of good energy transfer parameters and a higher Φ_{ov}, meaning a larger number of photons available for RET.

For Eu(TBP)−strep the optimal RET efficiency is accomplished for buffer B, mainly because of the shorter average donor−acceptor distance compared to the other buffers. Like for Tb**L,** the higher Φ_{ov} leads to a better LOD in buffer C. LODs for Eu(TBP) are lower compared to Eu**L**, which is mainly due to the better labeling ratio leading to a higher emission signal per streptavidin.

Time-Resolved Luminescence Microscopy. When a concentrated solution of Tb**L**−strep in pure water ([Tb**L**−strep] $> 10^{-5}$ M) was buffered at pH 8.3 with phosphate, the solution became cloudy and a solid could be isolated by centrifugation. Transmission microscopy observation of the solid in its mother liquor showed the formation of aggregates composed of balls of 1 to 2 microns in diameter (Figure 8).

Observation of these aggregates in fluorescence mode upon UV irradiation ($300 < \lambda_{exc} < 350$ nm), revealed a weak blue-green luminescence, characteristic of the Tb green emission with admixture of residual blue fluorescence from the proteins. Upon addition of Biot−QD (10^{-6} M) to the sample, no change could be observed immediately after addition, but within 1 h, the balls showed red fluorescence upon UV or visible ($550 < \lambda_{exc} < 600$ nm) irradiation (Figure 9), pointing to the accumulation of the dots at the surface of the balls, as a result of the avidin−biotin recognition process.

Interestingly, gated acquisition of the images showed very different behaviors depending on the excitation domain. When excited in the visible region ($550 < \lambda_{exc} < 600$ nm), that is directly into the QDs absorption bands, the fluorescence signals vanished as soon as a delay time, typically less than 50 μs, is imparted between excitation and acquisition, as expected on the basis of the short luminescence lifetimes of the nanocrystals.[45] In contrast, upon excitation into the UV domain ($300 < \lambda_{exc} < 350$ nm) while keeping all amplification parameters unchanged, a persisting signal could still be observed after the 50 μs delay time and even for longer delays up to hundred microseconds (Figure 10).

This long lasting signal, localized at the surface of the aggregates, is attributed to QD emission arising from Tb sensitization as a result of the efficient energy transfer process.

Conclusions

The present work clearly demonstrates that energy transfer to semiconductor nanocrystals is feasible using long-lived lanthanide complexes of terbium and europium as energy donors. This new approach provides an interesting combination in which both components bring their peculiar spectroscopic characteristic to afford an unprecedented time-resolved fluoro immunoassay format. The long-lived donors allowed for time-resolved acquisition of the energy transfer process, with a concomitant improvement of the detection sensitivity. The use of quantum dots as acceptors with their high extinction coefficients enlarged the scope of the recognition events through the increase of the Förster radius. While large absorptions of the dots first appeared as a drawback, providing undesired direct excitation of the acceptor, this inconvenience was largely

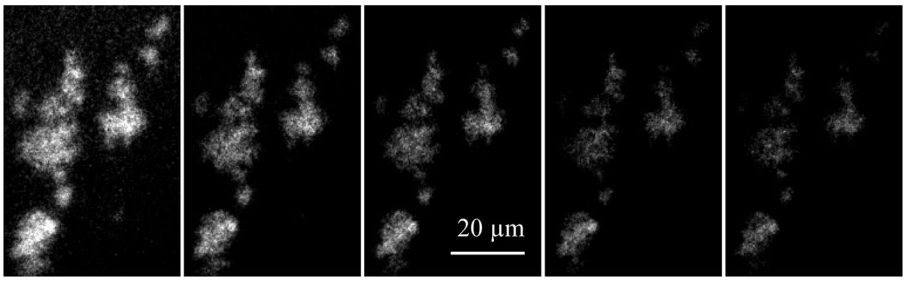

Figure 10. Time-gated luminescence spectra of the aggregates of Tb**L**−strep after incubation of Biot−QD (delay times $\delta = 50$, 80, 110, 140, and 170 s from left to right, $300 < \lambda_{exc} < 350$ nm, ×40 magnification).

compensated by the facts that ET to QD is detected at picomolar concentrations and that the gated acquisition eliminated spurious residual emission. Detection limits of 1.2×10^{-12} M for Biot−QD with Tb**L**−strep as donor could be accomplished in the immunoassay. The large R_0 values thereby obtained open interesting perspectives in the scope of recognition processes with the possibilities to study interactions within very large components. In particular, we realized a donor−acceptor pair with an R_0 value of more than 100 Å (104 Å for TbL−QD). The use of europium which emits in the red tail of the visible spectrum associated to quantum dots absorbing at even longer wavelengths can potentially also afford R_0 values larger than 100 Å, up to now only obtained with the help of genetically modified large fluorescent proteins.[16a] We also demonstrated that these couples are interesting targets in the frame of time-resolved luminescence microscopy, allowing for visualization of the ET process at the microscopic level.

The Lanthanide−QD systems afford very large perspectives in the frame of fluoro-immunoassays and biological analysis and demonstrated the physical availability of energy transfer to QD. Finally, one can also envisage to use different QDs of varying sizes and emission maxima to search for multiple recognition events with spectral and temporal discrimination, multiplexing,[51] which is of great interest in immunological science and economy, as several immuno markers can be detected within one measurement.

Experimental Section

Ln**L**−strep labeling was performed by mixing 0.5 mg of the sulfo-NHS activated ester of Ln**L**, Ln**L***[30,22] (dissolved in 2 μL DMSO), with 1 mg of streptavidin (Promega GmbH, High-Tech-Park, Schildkrötstr.15, D-68199 Mannheim, Germany) in 200 μL PBS buffer followed by dialysis for 1 day of incubation on a shaker at room temperature. Eu(TBP) labeled to streptavidin (Pierce Biotechnologie, Inc., P.O.Box 117, Rockford, IL 61105, USA) inside phosphate buffer containing BSA as well as Biot−APC (10 to 15 Biot/APC) were supplied by Cezanne SA, 280, Allée Graham Bell, Parc Scientifique Georges Besse, 30035 Nîmes cedex 1, France. Biot-QD (Qdot 655 Biotin Conjugate Trial Size Lot No. 0603−0050) were supplied by Quantum Dot Corp., 26118 Research Road, Hayward, CA 94545.

Time-Resolved Luminescence Titration of TbL**−Strep by Biot−QD.** In a typical resonance energy transfer experiment, a 2 mL solution of Tb**L**−strep (2.7×10^{-7} M) in 50 mM borate buffer (pH 8.3) containing 2% BSA and 0.05% NaN_3, was titrated by increasing amounts of Biot-QD (1×10^{-6} M) in the same buffer. After each addition of aliquots, the UV−vis spectra of the solution were recorded from 300 to 700 nm on a Uvikon 933 spectrometer to calculate the exact [Biot−QD]/[Tb**L**−strep] ratio assuming a labeling ratio of 3.7 Tb**L** dyes per streptavidin protein. For each addition, the time-resolved emission spectrum was recorded on a Perkin-Elmer LS50 spectrofluorimeter upon excitation at 308 nm after a delay of 250 μs and for a period of 750 μs. The intensity ratio between the intensity of emission of the acceptor (I_{660}) over that of the donor (I_{545}) was calculated and plotted versus the [Biot−QD]/[Tb**L**−strep] ratio.

Photophysical Spectroscopy. Steady-state fluorescence measurements were performed on Fluoromax3 fluorescence spectrometer (HORIBA Jobin Yvon GmbH, Chiemgaustr. 148, 81549 München, Germany). UV−vis absorption measurements were performed on Cary500 absorption spectrometer (Varian Inc., 3120 Hansen Way, Palo Alto, CA 94304-1030). FRET measurements were performed on a modified KRYPTOR system (Cezanne) for time-resolved integrated single photon counting at two photomultiplier channels (545 and 665 nm for Tb and 620 and 665 nm for Eu, filter based wavelength separation) with 2 μs integration steps over 8 ms using a fiber coupled vibrant Nd:YAG-OPO laser system (L.O.T.-Oriel GmbH & Co. KG, Im Tiefen See 58, D-64293 Darmstadt, Germany), 315 nm excitation wavelength, and 20 Hz repetition rate. QD as well as Ln decay time measurements were performed on an Andor iStar ICCD spectrometer setup (L.O.T.) with XeCl Excimer laser (Lambda Physik AG, Hans-Böckler-Strasse 12, D-37079 Göttingen, Germany) excitation and modified KRYPTOR system with fiber coupled vibrant Nd:YAG-OPO laser excitation.

Acknowledgment. This work was supported by the German Federal Ministry of Economics and Labour (InnoNet program 16N0225) and The French Centre National de la Recherche Scientifique. The authors acknowledge the help of Frank Sellrie, Universität Potsdam, for Ln**L**−strep labeling and purification and Dr Sophie Haebel, Universität Potsdam, for MALDI-TOF experiments as well as Cezanne SA (Nîmes) for provision of EuTBP−strep and Biot−APC.

Supporting Information Available: Luminescence decay times, τ_D, and lanthanide centered quantum yields, Φ_{Ln}, for Eu**L**−strep, Tb**L**−strep, and Eu(TBP)−strep in different buffering media (Table T1); overlap integrals J_λ and Förster radii R_0 of the donor−acceptor pairs with Biot-QD as acceptor (Table T2); MALDI-TOF spectra of streptavidin and its three lanthanide bioconjugates as well as UV−vis spectra of the Ln complexes, streptavidin, and Ln−strep (Figure S1); influence of azide concentration on Tb**L**−NHS and Tb**L**−strep luminescence decay time (Figures S2 and S3); relative luminescence intensities of Eu**L**−strep, and Tb**L**−strep as a function of added BSA (Figure S4); and control experiments for dynamic energy transfer between Tb**L**, Eu**L**, and Eu(TBP) with Biot−QD (Figures S5−S7) and between Eu(TBP) and Biot−(APC) (Figure S8). This material is available free of charge via the Internet at http://pubs.acs.org.

JA062693A

(50) Hendrickson, W. A.; Pähler, A.; Smith, J. L.; Satow, Y.; Merritt, E. A.; Phizackerley, R. P. *Proc. Natl. Acad. Sci. U.S.A.* **1989**, *86*, 2190.
(51) Clapp, A. R.; Medintz, I. L.; Uyeda, H. T.; Fisher, B. R.; Goldman, E. R.; Bawendi, M. G.; Mattoussi, H. *J. Am. Chem. Soc.* **2005**, *127*, 18212.